970 *Biochemistry* **2011,** *50,* 970–980
DOI: 10.1021/bi101738w

BIOCHEMISTRY
including biophysical chemistry & molecular biology
Article

Amplitude Spectrum of Structural Fluctuations in Proteins from the Internal Diffusion of Solutes of Increasing Molecular Size: A Trp Phosphorescence Quenching Study

Giovanni B. Strambini* and Margherita Gonnelli

Consiglio Nazionale delle Ricerche, Istituto di Biofisica, 56124 Pisa, Italy

Received October 29, 2010; Revised Manuscript Received December 13, 2010

ABSTRACT: The accessibility of O_2, acrylamide, and four acrylamide derivatives of increasing molecular size {*N*-(hydroxymethyl)acrylamide, *N*,*N*′-methylene-bisacrylamide, *N*-[tris(hydroxymethyl)methyl]acrylamide, and 2-acrylamido-2-methyl-1-propanesulfonic acid} to buried Trp residues in four proteins, as determined by dynamic quenching of their phosphorescence emission, was utilized for probing the amplitude range of structural fluctuations in these macromolecules. The quenching rate constant of each solute, k_q, was determined (at 25 and −5 °C) for liver alcohol dehydrogenase, glyceraldehyde-3-phosphate dehydrogenase, azurin, and alkaline phosphatase. The results show that high-frequency small amplitude motions pervade the protein globular fold, permitting relatively unhindered diffusion of small diatomic molecules all the way to compact cores of the macromolecule. For larger solutes, the access to deep regions drops sharply with molecular size, with acrylamide probably representing a threshold for diffusion of a solute through homogeneous compact domains, on the long second time scale. The results emphasize the variability in the amplitude of protein motions between deep cores and more superficial regions of the globular fold and unveil the existence of unexpectedly large amplitude low-activation barrier fluctuations permitting the penetration of solutes with comparatively large M_w values.

There is a growing awareness that protein dynamics is intimately correlated to biological function. More recently, particular attention has been drawn to slow collective motions in the submicrosecond to second time domain as there is mounting evidence that structural fluctuations on this time scale are directly linked to enzymatic catalysis, signal transduction, and protein−protein interactions (*1*−*7*). Despite the relevance to biological function, the amplitude spectrum of slow motions in globular proteins is still poorly characterized. As a result, little is known about the intrinsic variability of protein motions among globular folds, their correlation to secondary and tertiary structure, and the extent to which they are modulated by bound ligands or medium conditions. This paucity of data is caused to the experimental difficulties associated with the detection of slow motions (*6*, *8*−*10*), especially when dealing with transitions to rarely populated conformational substates that, nevertheless, may be functionally important.

The diffusion of inert solutes through globular proteins requires structural fluctuations that lead to transient formation of channels or the opening of gates of proportionate size. Therefore, by studying the rate of migration of solutes with progressively larger molecular weights to internal protein sites, we may be able to gain insight into the time scale and amplitude range of protein motions. One approach is to monitor the quenching of Trp luminescence of internal residues by the penetration of quenching solutes, Qs, varying in molecular size. The technique, initially applied to quenching of Trp fluorescence on the nanosecond time scale (*11*), was subsequently extended to the long-lived phosphorescence emission, in that way expanding the range of measurable diffusion rates to the microsecond to second time domain (*12*−*20*). Quenching studies measure the phosphorescence lifetime, τ, as a function of the quencher concentration, [Q], and evaluate the bimolecular quenching rate constant, k_q, from the gradient of the Stern−Volmer plot

$$1/\tau = 1/\tau_0 + k_q[Q] \quad (1)$$

where τ_0 is the unperturbed lifetime. For efficient quenching of Trp free in solution, k_q is close to the diffusion-limited rate constant k_d, where $k_d = 4\pi r_0 D$ (r_0 is the sum of molecular radii and D the sum of the individual diffusion coefficients). With buried Trp residues in proteins, k_q may fall even by several orders of magnitude (*14*), reflecting the slower diffusion of Q through the protein matrix, relative to diffusion in water.

To date, a systematic study of the dependence of penetration rates on Q size has not been performed on any protein. Phosphorescence quenching experiments have been mainly concerned with small diatomic and triatomic molecules (e.g., O_2, NO, and CS_2) and only more recently with lager acrylonitrile (M_w = 53) (*21*)and acrylamide (*14*)(M_w = 71). Whereas diatomic molecules readily penetrate the protein matrix, internal diffusion of acrylamide, which is approximately twice the size of O_2, can be strongly inhibited and may vary by several orders of magnitude among protein sites (*14*). Apparently, in some proteins, its access is regulated by protein gates (*19*), while in some compact protein cores, quenching is barely detectable on the second time scale. Knowledge of the penetration of even larger Qs and whether there is a size cutoff beyond which internal regions ought to be considered inaccessible to solutes, least of polypeptide unfolding, is totally lacking. This investigation aims to make a systematic comparison of Q penetration rates as a function of

*To whom correspondence should be addressed: CNR, Istituto di Biofisica, Area della Ricerca, via Moruzzi 1, 56124 Pisa, Italy. Telephone: +39 050 315 3046. Fax: +39 050 315 2760. E-mail: strambini@pi.ibf.cnr.it.

 Published on Web 01/10/2011

Q size, extending the measurable amplitude range of structural fluctuations by introducing novel quenchers with increasing M_w values, up to 3 times that of acrylamide.

In the selection of quenching solutes, a basic requisite is that the quencher−chromophore interaction be short-range as it prevents the possibility that quenching by long-range through-space interactions with Q in the solvent competes with and masks the migration of Q through the protein matrix. The magnitude of the external quenching rate may be estimated from knowledge of the distance dependence of the quenching interaction, $k(r)$. Among current quenchers, $k(r)$ has been determined for only acrylamide and acrylonitrile (*14*, *21*). It indicates that with these moieties through-space quenching is relatively short-range and that the interaction with Q in the solvent is practically negligible when Trp residues are buried more than a couple of angstroms below the molecular surface (*14*). Consequently, acrylamide derivatives in which the quenching moiety is linked to neutral or charged groups with variable molecular weights should provide suitable quenchers for spanning a wide range of Q sizes.

This report examines the quenching rate of four commercially available acrylamide derivatives with increasing M_w values, namely, *N*-(hydroxymethyl)acrylamide [HA[1] (M_w = 101)], *N*,*N*′-methylene-bisacrylamide [BA (M_w = 154)], *N*-[tris(hydroxymethyl)methyl]acrylamide [TA (M_w = 175)], and 2-acrylamido-2-methyl-1-propanesulfonic acid sodium salt [SA (M_w = 206)]. By comparing k_q values over a wide range of Q sizes (from O_2 to SA), in four distinct protein sites, we enquire about the intrinsic variability of the amplitude spectrum of protein motions, its possible correlation to structural data such as depth of burial and local secondary and tertiary structure, and the sensitivity of specific motions to binding of ligands, such as coenzymes and metal ions. While the dependence on temperature will provide indications about the activation barrier associated with specific amplitudes, differences between neutral and charged quenchers may indicate whether these motions open internal sites to the solvent. The following proteins were chosen: liver alcohol dehydrogenase (LADH), glyceraldehyde-3-phosphate dehydrogenase (GAPDH), azurin, and alkaline phosphatase (AP). All exhibit long-lived phosphorescence from a single Trp residue (*22*) shielded from the aqueous interface by a protein spacer ranging in thickness from 0.45 to 1.1 nm. The results emphasize the great site to site variability in the time scale and amplitude range of protein motions and unveil unsuspected large amplitude low-barrier fluctuations involving ordered regions of the globular fold.

MATERIALS AND METHODS

All chemicals were of the highest purity grade available from commercial sources and unless specified to the contrary were used without further purification. Acrylamide (99.9% electrophoretic purity) was from Bio-Rad Laboratories (Richmond, CA). Ultrapure, MB grade *N*,*N*′-methylene-bisacrylamide (BA) was from USB Corp. (Cleveland, OH). *N*-(Hydroxymethyl)-acrylamide (HA) (>98%) was from TCI Europe (Zwijndrecht, Belgium). ADPR, *N*-[tris(hydroxymethyl)methyl]acrylamide (TA) (93%), and 2-acrylamido-2-methyl-1-propanesulfonic acid sodium salt (SA) were from Sigma-Aldrich. Tris(hydroxymethyl)-aminomethane (Tris), spectral grade glycerol, and NaCl Suprapur were from Merck (Darmstadt, Germany). Water was purified by reverse osmosis (Milli-RX 20, Millipore, Billerica, MA) and subsequently passed through a Milli-Q Plus system (Millipore Corp., Bedford, MA). The protein horse liver alcohol dehydrogenase (LADH), supplied by Fluka Chemie GmbH, and alkaline phosphatase (AP) from *Escherichia coli* were purchased from Sigma-Aldrich. Glyceraldehyde-3-phosphate dehydrogenase (GAPDH) from *Bacillus stearothermophilus* was kindly supplied by G. Branlant (University Henri Poincaré, Nancy, France). Wild-type azurin from *Pseudomonas aeruginosa* was prepared from the plasmid carrying the wild-type sequence, supplied by A. Desideri (University of Rome "Tor Vergata", Rome, Italy), following a procedure analogous to that described by Karlsson et al. (*23*). The azurin mutant C112S was prepared following the same procedure as for the wild-type protein except for the omission of any addition of $CuSO_4$ in both growth and purification medium. The C112S mutant was constructed using the QuikChange kit (Stratagene, La Jolla, CA) and confirmed by sequencing.

Lately, LADH has not been commercially available, and the crystalline suspension used in these experiments was approximately 2−3 years old. As is standard practice with older supplies, before each set of experiments, the solubilized protein was tested for integrity. A fully native state was confirmed by electrophoresis, the spectroscopic (absorption, fluorescence, and phosphorescence) characteristics, and the enzymatic activity. A typical sodium dodecyl sulfate−polyacrylamide gel electrophoresis (SDS−PAGE) chromatogram is supplied as Supporting Information. To remove NAD^+ from GAPDH, we treated the enzyme with activated charcoal as reported previously (*24*). Copper-free azurin (apo-azurin) was prepared from holo-azurin by adding 0.1 M potassium cyanide and 1 mM EDTA in 0.15 M Tris-HCl (pH 8), followed by column chromatography (*25*). Zn-azurin was formed from apo-azurin by the addition of $ZnCl_2$ at a molar ratio of 2:1 (*26*). mdAP is a Zn-depleted form of AP prepared by dialysis of the native protein in the presence of 20 mM EDTA for 3 h, followed by dialysis with pure buffer. Full recovery of native AP, as monitored by the characteristically long phosphorescence lifetime, was obtained within 1 h of incubating mdAP in 2 mM $ZnCl_2$.

For phosphorescence measurements in fluid aqueous solutions, protein samples were placed in appositely constructed, 5 mm × 5 mm, quartz cuvettes with a leakproof capping designed to allow thorough removal of O_2 by the alternating application of moderate vacuum and inlet of ultrapure N_2 (*27*). With viscous, glycerol-containing samples, removal of O_2 required prolonged equilibration times, up to 3 h. Phosphorescence measurements were conducted at a protein concentration that ranged between 2 and 10 μM, unless otherwise specified.

Phosphorescence Measurements. Phosphorescence spectra and decays were measured with pulsed excitation on a homemade apparatus (*19*, *27*). The exciting light (λ_{ex} = 292 nm) was provided by a frequency-doubled Nd/Yag-pumped dye laser (Quanta Systems, Milan, Italy) with a pulse duration of 5 ns and a typical energy per pulse of ~0.05 mJ. For decay measurements, the phosphorescence intensity was collected at 90° from vertical excitation through a filter combination with a transmission window of 405−445 nm (WG405, Lot-Oriel, Milan, Italy; with an interference filter, DT-Blau, Balzer, Milan, Italy) and monitored

[1]Abbreviations: HA, *N*-(hydroxymethyl)acrylamide; BA, *N*,*N*′-methylene-bisacrylamide; TA, *N*-[tris(hydroxymethyl)methyl]acrylamide; SA, 2-acrylamido-2-methyl-1-propanesulfonic acid sodium salt; LADH, liver alcohol dehydrogenase; GAPDH, glyceraldehyde-3-phosphate dehydrogenase; AP, alkaline phosphatase; mdAP, Zn-depleted alkaline phosphatase; Znaz, Zn-azurin; Caz, C112S azurin mutant; ADPR, adenine diphosphate ribose.

by a photomultiplier (EMI 9235QA). The prompt Trp fluorescence intensity from the same pulse was used to account for possible variations in the laser output between measurements, as well as to obtain fluorescence-normalized phosphorescence intensities. A decrease in the latter would indicate partial quenching of phosphorescence during the dead time of these measurements, as for example in the case of static interaction with closely bound quenchers. All phosphorescence decays were analyzed in terms of discrete exponential components by a nonlinear least-squares fitting algorithm (DAS6, Fluorescence decay analysis software, Horiba Jobin Yvon, Milan, Italy).

Quenching Experiments. Quenching experiments were conducted by measuring the phosphorescence lifetime, τ, of protein samples as a function of the quencher concentration, [Q], in solutions (*14*), and the bimolecular quenching rate constant, k_q, was derived from the gradient of the Stern−Volmer plot (eq 1). In the case of LADH, the phosphorescence decay is intrinsically heterogeneous and tends to remains so even when the average phosphorescence lifetime is markedly reduced by quenching. Because in all the proteins examined the emission is due to a single Trp residue per subunit, such lifetime heterogeneity reflects the presence of more than one stable conformation of the macromolecule (*28*), each with its distinct τ_0 and quenching rate constant. For the sake of convenience, and also because an evaluation of individual quenching rates is model-dependent, lifetime Stern−Volmer plots were all constructed from the intensity-averaged lifetime (*29*) ($\tau_{av} = \sum\alpha_i\tau_i^2/\sum\alpha_i\tau_i$), obtained in general from a biexponential fit of phosphorescence decays. Thus, the value of k_q derived from the gradient of these plots is an average quantity.

Acrylamide and acrylamide derivative stocks solutions were prepared daily by dilution of the commercial supply in the same buffer utilized with each protein system. The following buffers were used: 20 mM Tris-HCl (pH 7) for LADH and AP, 30 mM sodium acetate with 1 mM EDTA (pH 5.5) for azurin, and 30 mM potassium phosphate with 1 mM EDTA (pH 7.4) for GAPDH. With negatively charged SA and with TA, whose stock supply contains 7% KCl, the ionic strength was kept constant at 0.31 M by addition of KCl to the respective buffer. The LADH−ADPR complex was formed by the addition of 0.8 mM ADPR to a solution of LADH. In general, the maximal [Q] was dictated by either the solubility of Q (see BA) or the lifetime resolution of the apparatus (quenching rates of $\leq 2 \times 10^4$ s^{-1}). For each quencher concentration, at least three independent samples were analyzed, and the reported results represent the mean lifetime value. The reproducibility of phosphorescence lifetime measurements was generally better that 7%. With O_2 quenching, the highest concentration employed was that of an aqueous solution in equilibrium with the atmosphere, as derived from the solubility of O_2 at various temperatures (e.g., 258 μM at 25 °C). Lower O_2 concentrations were determined directly from the lifetime of alkaline phosphatase (AP) added to the protein sample under examination, as described previously (*18*). The reference $k_q(O_2)$ values of AP are 1.7×10^6 and 2.3×10^5 M^{-1} s^{-1} at 25 and −5 °C, respectively.

Fitting of quenching rates to theoretical models was conducted with Origin.

Quenching Models. Quenching of the luminescence of Trp residues in proteins by small solutes (Q) in solution has been analyzed in terms of mechanisms that involve either diffusion of Q to the protein surface followed by long-range interactions with the buried chromophore (external quenching) or diffusive penetration of Q through the protein matrix into its proximity. Pertinent analytical expressions for the quenching rate, obtained by solving Fick's diffusion equation applying radiation boundary conditions, and their application range in the realm of protein phosphorescence have been discussed in detail previously (*30*). Briefly, by neglecting a transient time-dependent term arising from Q molecules already in the proximity of the chromophore at the instant of excitation, we find the steady state bimolecular quenching rate constant, k_q, is given by

$$k_q = k_D k_I/(k_D + k_I) \quad (2)$$

where k_D ($=4\pi aD$) is the Smoluchowski diffusion-controlled rate constant, k_I ($=4\pi a^2 B$) is the diffusion-independent maximum rate constant, and D is the sum of the separate diffusion coefficients of Q and protein in solution. B is an interaction strength parameter related to the distance dependence of the quenching interaction, $k(r)$, and a is the distance (from center to center) of closest approach between Q and the chromophore. Depending on which of the two rate constants is smaller, the process goes from the diffusion-controlled regime ($k_D \ll k_I$; $k_q = k_D \propto D$) to the reaction-controlled regime ($k_D \gg k_I$; $k_q = k_I$), where k_q is independent of diffusion.

For diffusive penetration of Q across a protein shell with a thickness T, characterized by a diffusion constant $D_p \ll D$, the process is bound to be under diffusion control, and in such a case, the rate constant assumes the form of a corrected Smoluchowski equation (*30*, *31*)

$$k_q(\text{penetration}) = 4\pi aDp(1 + a/T) \quad (3)$$

where now a is the radius of the impermeable protein core surrounding the chromophore. In the special case in which internal diffusion is dominated by a slow rate-limiting conformational transition (e.g., partial unfolding), opening a channel to the buried chromophore, the rate constant reduces to (*19*)

$$k_q(\text{gate}) = k_o/([Q] + \sigma) \quad (4)$$

where k_o is the opening rate and σ is the [Q] corresponding to midpoint saturation of the gate. $\sigma = k_c/k_q'$, where k_c is the gate closing (refolding) rate and k_q' is the bimolecular quenching rate constant of the protein in the "open gate" configuration.

External quenching of protein phosphorescence by freely diffusing Q in the aqueous phase was recently shown to rigorously comply with the rapid diffusion limit (RDL) regime (*32*). The bimolecular rate constant, k_I(RDL), derived for an essentially flat protein surface and an exponential distance dependence of the interaction {$k(r) = k_0 \exp[-(r - r_0)/r_e]$, where r_0 is the center to center distance between Q and the chromophore in van der Waals contact} decreases with the thickness of the protein spacer (r_p) separating the chromophore from the aqueous interface ($r_p + r_0 = a$ is the shortest center-to-center distance between the internal chromophore and Q at the aqueous interface) according to (*33*)

$$k_I(\text{RDL}) = k_I(r_p) = 2\pi N \times 10^{-3}[(r_p + r_0)r_e^2 + 2r_e^3]k_0 \exp(-r_p/r_e) \quad \text{M}^{-1}\,\text{s}^{-1} \quad (5)$$

where N is Avogadro's number and r_e is the attenuation length (r_e and r_p in centimeters). For acrylamide, $k_0 = 3.5 \times 10^{10}$ M^{-1} s^{-1}, $r_e = 0.29$ Å, and $r_0 = 5$ Å (*14*, *32*). An additional contribution to external quenching may come from Q binding to the protein surface (rapid and reversible binding with a dissociation constant K_d),

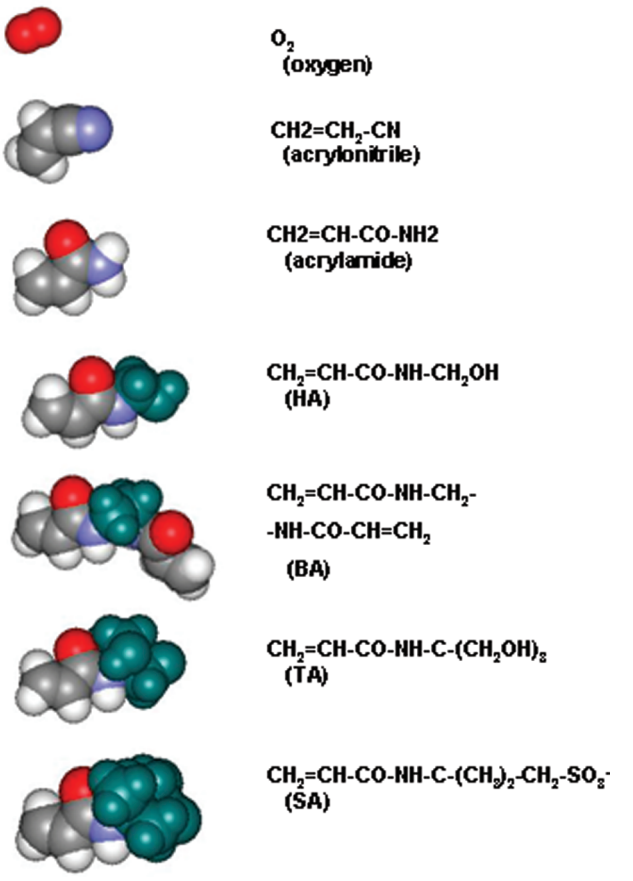

FIGURE 1: Space filling model and chemical formula of quenching solutes considered in this study.

which is given by (*19*)

$$k_q(\text{binding}) = k(r')/([Q] + K_d) \quad (6)$$

where $k(r')$ is the quenching rate of Q bound a distance r' from the chromophore.

It should be emphasized that the contributions from gating and binding saturate at high Q concentrations. Consequently, these processes will give rise to nonlinear, hyperbolic Stern−Volmer plots, a signature that helps to distinguish them from other quenching mechanisms.

RESULTS

The objective of this investigation is to compare the penetration rate of quenching solutes of various molecular sizes to internal Trp sites of LADH, GAPDH, azurin, and AP (Figure 1). The quencher series under consideration comprises O_2, acrylonitrile (AN), acrylamide, HA, BA, TA, and SA, spanning a range in M_w from 32 to 206. AN quenching of these proteins has recently been found (*21*). Data for O_2 and acrylamide are also available, but these data often refer to different experimental conditions. To have a uniform set of data, at 25 and −5 °C, O_2 and acrylamide quenching experiments, when necessary, were repeated.

LADH. Trp-314 of LADH is located at the dimer subunit interface, separated from the solvent by a protein spacer that is at least 0.45 nm thick (*34*). The indole side chain is sandwiched between two β-sheets that extend across the subunit interface, giving rise to a relatively rigid local structure. As a result, the chromophore exhibits long-lived phosphorescence in fluid solutions with average lifetimes, τ_0, of 0.42 s at 25 °C and 2.5 s at −5 °C. At a high ionic strength (0.31 M), τ_0 decreases to 0.23 and 0.97 s,

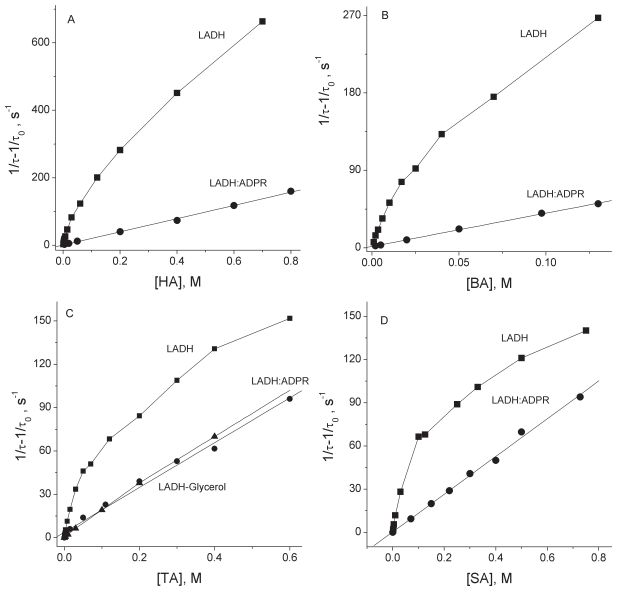

FIGURE 2: Lifetime Stern−Volmer plots relative to the quenching of LADH (■) and LADH/ADPR (●) phosphorescence by four acrylamide derivatives, at 25 °C: (A) HA, (B) BA, (C) TA, and (D) SA. Also included in panel C is TA quenching of LADH in a glycerol/buffer mixture (68:32, w/w) (▲). The line drawn through the points (● and ▲) is a linear fit of the data. Each point is the mean value of at least three separate determinations. Deviations from the mean are typically smaller than 5%.

respectively. Quenching experiments were conducted with O_2, HA, BA, TA, and SA.

O_2 quenching, up to quenching rates of $\approx 2 \times 10^4$ s^{-1}, yielded linear lifetime Stern−Volmer plots (Figure S2 of the Supporting Information) whose gradient gave bimolecular rate constants, $k_q(O_2)$, of 4.5×10^7 M^{-1} s^{-1} at 25 °C and 7×10^6 M^{-1} s^{-1} at −5 °C. The data are in good accord with the previously reported value of 3.7×10^7 M^{-1} s^{-1} at 20 °C.

The acrylamide derivatives HA, BA, TA, and SA quenched the emission of LADH, leading in every case to a progressive shortening of the phosphorescence lifetime, which is typical of dynamic quenching reactions. However, the quenching rate of these large solutes is markedly nonlinear with respect to Q concentration, the downward curving Stern−Volmer plots, reported in Figure 2, indicating that the reaction tends to saturate at high quencher concentrations. A similar trend was previously observed with acrylamide (*19*), but not with smaller O_2 and AN. The decrease in quenching effectiveness as obtained by dividing the quenching rate by Q concentration is illustrated in Figure 3, where it is compared to that reported for acrylamide. Although, relative to the latter, there is a significant attenuation of the quenching efficiency of larger derivatives, the trend does not follow a smooth inverse dependence on Q size. From acrylamide to SA, the maximum value of k_q, k_{qmax}, which refers to dilute solutions, decreases by ~16-fold even if the rate constant of BA ($M_w = 154$) is approximately twice that of HA ($M_w = 101$) and is not markedly different between TA and SA.

The profiles of Figure 3 are characterized by a monophasic decrease in k_q in the 10−100 mM concentration range. Previously, the saturation behavior of acrylamide was attributed to protein-gated quencher penetration, and the data were fit in terms of two separate gates (eq 4) with frequencies of 40 and 1.1×10^4 s^{-1} at 25 °C (*19*). For the acrylamide derivatives listed above, all k_q profiles were adequately fitted (Figure 3) by a single-gate

model (eq 4) with a linear component [the constant c (Table 1)], and the gate frequency, k_0, and corresponding saturation midpoint, σ, are reported in Table 1. The constant c accounts for any possible linear contribution to the overall quenching reaction. These contributions may arise from (i) quenching impurities, Im, in the acrylamide derivative stocks (e.g., additives that block polymerization) acting by long-range interactions with Im in the solvent (eq 5), (ii) a residual through-space quenching by Q itself in the solvent (eq 5), and (iii) additional Q quenching routes, such as a high-frequency gate, or weak binding, neither of which saturates in the experimental Q concentration range (i.e., $[Q]_{max} < \sigma$ or K_d). These contributions range from 5 to 18% of the maximum quenching rate, k_{qmax} ($k_{qmax} = k_0/\sigma + c$), and were found to vary substantially among commercial supplies.

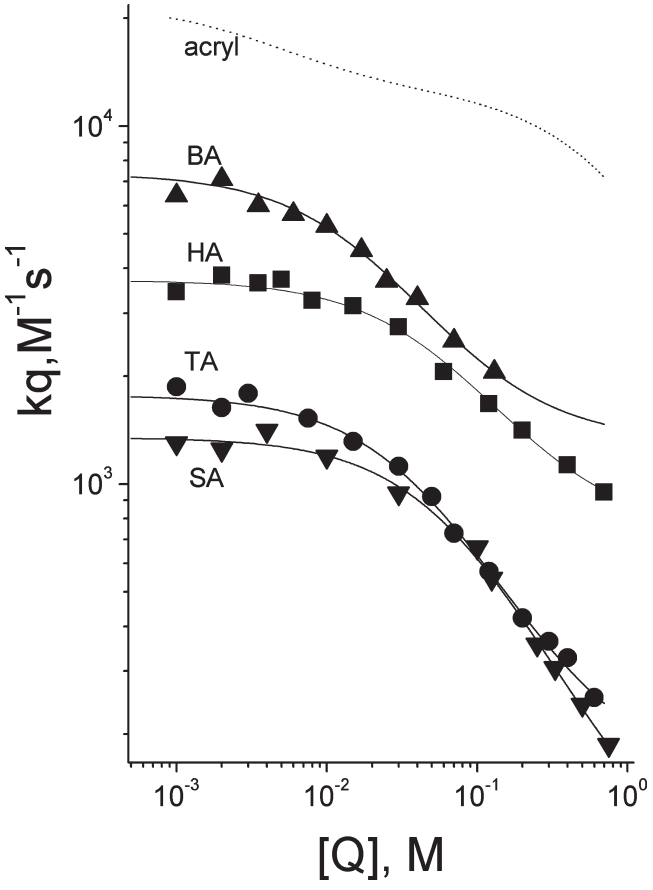

FIGURE 3: Quenching of LADH phosphorescence in buffer by HA (■), BA (▲), TA (●), and SA (▼) at 25 °C. Dependence of the bimolecular quenching rate constant, k_q, on the concentration of the four acrylamide derivatives as obtained by dividing the quenching rate ($1/\tau - 1/\tau_0$) of Figure 2 by Q concentration. The solid line through the points is the best fit of the data to one gate (eq 4) plus a constant. The dotted line, representing the corresponding acrylamide data (*19*), is included as a reference.

The similarity in k_0 values among acrylamide derivatives would indicate that access to the site of Trp-314, or to its proximity, by these large solutes is dominated by a slow structural fluctuation in the frequency range of 70−170 s^{-1}, presumably opening a gate common to all quenchers. The 2-fold increase in k_0/σ from HA to BA appears to be correlated to the reduction in σ ($\sigma = k_c/k_q'$). If one assumes a constant gate closing rate (k_c), then the maximal quenching efficiency of the putative gate would be largely determined by the open gate quenching rate constant, k_q'. In this hypothesis, the greater quenching efficiency of BA relative to that of HA would be ascribed to the predicted 2-fold increase in k_q' for double-headed BA.

When the temperature is decreased to −5 °C, all quenching reactions are significantly slowed, but the shape of Stern−Volmer plots remains totally analogous to that observed at 25 °C. These plots are equally well fitted in terms of a single-gate model, and as indicated in Table 1, the main effect of lowering the temperature is a major reduction in the gate frequency. The gate frequency activation enthalpy, $\Delta H^{\ddagger}(k_0)$, estimated from the two-point Arrhenius plot (Table 1) falls in the 7−12 kcal/mol range. We recall that both the frequency and the activation barrier of the putative gate approach the values derived for the slow gate in acrylamide quenching (*19*), which might be suggestive of a common penetration pathway.

To test whether a reduction in LADH flexibility would affect the internal migration of these solutes, the quenching experiments described above were repeated on the binary complex with the coenzyme analogue ADPR. On the basis of the B factors, the increase in τ_0 (*35*), and the enhanced thermal stability (*36*), the binary complex is significantly more rigid than the free protein. For the rest, the crystallographic structure shows that in the complex the protein maintains the open state conformation of the free protein (*34*, *37*) and that in the region of the dimer interface, where Trp-314 is located, the structure is totally unchanged by formation of the complex.

The O_2 quenching rate constant of the complex decreased by ~25% (at 25 °C), relative to that of LADH, whereas the corresponding activation enthalpy, $\Delta H^{\ddagger}(k_q)$, derived from the slope of the two-point Arrhenius plot {$\ln[k_q(T)]$ vs $1/T$} (*37*), increased by 1.7 kcal/mol (Table 2), findings consistent with a more rigid fold at the subunit interface. Formation of the

Table 1: Gate Parameters Relative to the Quenching of LADH Phosphorescence by Acrylamide Derivatives

quencher	k_0 (s^{-1})	σ (M)	k_0/σ (M^{-1} s^{-1})	c (s^{-1})	$\Delta H^{\ddagger}(k_0)$ (kcal/mol)
			T = 25 °C		
HA	173 ± 39	0.058 ± 0.016	2941	730 ± 158	8.7
BA	109 ± 42	0.018 ± 0.009	5886	1317 ± 270	8.2
TA	68 ± 24	0.042 ± 0.028	1656	152 ± 46	12.0
SA	96 ± 24	0.075 ± 0.022	1280	69 ± 39	6.7
			T = −5 °C		
HA	33 ± 16	0.059 ± 0.026	561	103 ± 28	
BA	20 ± 17	0.02 ± 0.02	1020	115 ± 122	
TA	7 ± 5	0.017 ± 0.01	413	27 ± 12	
SA	28 ± 17	0.110 ± 0.05	252	11 ± 7	

Table 2: Bimolecular Phosphorescence Quenching Rate Constants (k_q or k_{qmax}), at 25 °C, and Corresponding Activation Enthalpies ($\Delta H^{\ddagger}$) of Selected Proteins by Solutes Q of Variable Molecular Sizes[a]

sample	O_2	AN[b]	acrylamide	HA	BA	TA	SA
			k_q (M^{-1} s^{-1})				
LADH	4.5×10^7	4.2×10^5	$\underline{2.1 \times 10^4}$	$\underline{3.7 \times 10^3}$	$\underline{7.2 \times 10^3}$	$\underline{1.8 \times 10^3}$	$\underline{1.3 \times 10^3}$
LADH−ADPR	3.4×10^7	1.2×10^5	1.2×10^3	1.9×10^2	3.9×10^2	1.6×10^2	1.3×10^2
LADH in glycerol	−	−	3.2×10^3	−	−	1.9×10^2	−
GAPDH	7.9×10^7	6.2×10^6	2.6×10^6	1.3×10^6	7.8×10^5	5.7×10^4	1.3×10^4
Zn-azurin	1.3×10^7	3.1×10^3	1.5×10^0	2.7×10^0	5.0×10^{-1}	−	−
C112S-azurin	2.0×10^7	5.7×10^3	6.6×10	2.5×10	3.8×10	1.1×10	9.4×10^0
AP	1.7×10^6	1.4×10^2	1.0×10^{-1}	−	−	−	−
mdAP	1.9×10^6	9.8×10^2	6.0×10	−	−	−	−
			$\Delta H^{\ddagger}$ (kcal/mol)				
LADH	10.8	12.24	$\underline{8.5}$	$\underline{9.0}$	$\underline{9.8}$	$\underline{7.5}$	$\underline{8.7}$
LADH−ADPR	12.5	14.9	12.9	12.8	12.0	10.9	8.9
LADH in glycerol	−	−	17.6	−	−	10.5	−
GAPDH	8.6	13.2	9.9	10.3	9.9	10.2	10.7
Zn-azurin	10.0	12.2	10.4	4.0	3.7	−	−
C112S-azurin	9.4	14.1	17.7	15.5	16.3	5.7	4.4
AP	10.6	16.5	22.0	−	−	−	−
mdAP	10.3	16.4	25.4	−	−	−	−

[a]Underlined k_q and $\Delta H^{\ddagger}$ values refer to $k_{qmax} = k_0/\sigma + c$ and to the temperature dependence of k_{qmax}, respectively. [b]Data from ref *21*.

complex caused a major attenuation of the quenching rate of acrylamide derivatives, as illustrated by the lifetime Stern−Volmer plots in Figure 2. Not only are the rates of quenching significantly reduced in the coenzyme complex (from 20-fold with HA to 10-fold with SA), but the Stern−Volmer plots now are also essentially linear with respect to quencher concentration, throughout. Unpredictably, the residual quenching rate is now similar among the derivatives [$k_q = 130-190$ M^{-1} s^{-1} (Table 2)], with the exception of a 2-fold larger rate for double-headed BA ($k_q = 390$ M^{-1} s^{-1}). Evidently, access to the proximity of Trp-314 of quenchers the size of HA and larger is strongly inhibited in the complex, and presumably, the residual rate of quenching represents an external contribution from either a weak association of Q with the protein ($K_d > 2$ M), which would explain the 2-fold increase in k_q with BA, or impurities in commercial supplies. Of course, any "spurious" quenching will be present also with LADH, where it will contribute to the linear component, the constant c, which in fact is comparable in magnitude in the cases of TA and SA.

External quenching falls under the reaction control regime, and it was shown to be insensitive to solvent viscosity (*32*). A test conducted on TA quenching of LADH in 68% glycerol/water (w/w) solutions demonstrated that the increase in solvent viscosity (17.7-fold at 25 °C and 35.5-fold at −5 °C) (*19*) has virtually the same effect as formation of the complex (Figure 2). The Stern−Volmer plot becomes linear with respect to Q concentration and yields a k_q(TA) value of 189 M^{-1} s^{-1}, at 25 °C. It would seem that both in viscous solution and in the LADH−ADPR complex, TA penetration of LADH is blocked and the residual quenching reaction represents an external contribution that is independent of solvent viscosity.

GAPDH. The protein is a tetramer, and the phosphorescence probe, Trp-84, is located far from the subunit contact region, buried at least 0.5 nm below the molecular surface (*38*). The phosphorescence decay is well represented by a single lifetime, τ_0, of 72 ms at 25 °C and 453 ms at −5 °C. Quenching experiments were conducted with O_2, HA, BA, TA, and SA.

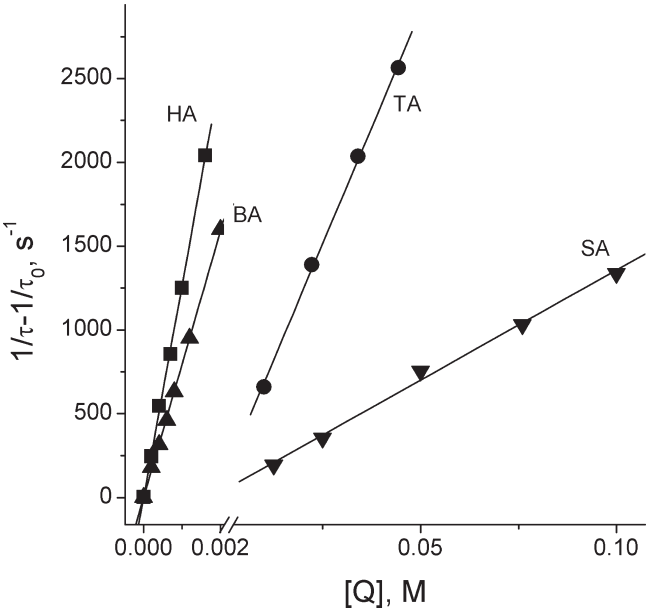

FIGURE 4: Lifetime Stern−Volmer plots for quenching of GAPDH phosphorescence by HA (■), BA (▲), TA (●), and SA (▼), at 25 °C. The line drawn through the points is a linear fit of the data. Each point is the mean value of at least three separate determinations. Deviations from the mean are typically smaller than 7%.

O_2 quenching was found to be more efficient than in LADH, the linear Stern−Volmer plot (Figure S2 of the Supporting Information) yielding bimolecular quenching constants, $k_q(O_2)$, of 7.9×10^7 M^{-1} s^{-1} at 25 °C and 1.6×10^7 M^{-1} s^{-1} at −5 °C. Among buried Trp residues in proteins, this value is second only to the value of 1.4×10^8 M^{-1} s^{-1} for superficial Trp-59 in RNase T1 (*39*).

The acrylamide derivatives are also unexpectedly efficient quenchers, and $1/\tau$ is linear with respect to Q concentration throughout. The Stern−Volmer plots of HA, BA, TA, and SA are displayed in Figure 4, and the values of k_q derived from the

slope are listed in Table 2, together with the respective activation barriers, $\Delta H^{\ddagger}(k_q)$. We note that the quenching constants are relatively large, $>10^4$ M^{-1} s^{-1}, and exhibit a smooth inverse dependence on Q size, k_q decreasing by a factor of 100 from HA to SA. The value of $\Delta H^{\ddagger}(k_q)$ is $\approx$10 kcal/mol, practically constant among different size solutes. The rather low and constant activation barrier to the internal diffusion of these solutes suggests that perhaps the same structural fluctuations are involved in the migration process.

Azurin. Trp-48 of azurin is located in the compact core of the 14 kDa macromolecule, buried at least 0.8 nm below the molecular surface (*40*, *41*). In the native form, its phosphorescence emission is fully quenched by the interaction with bound Cu. Here, we examined the wild-type protein in which Cu has been substituted with Zn (Znaz) and a metal-free form obtained with the C112S mutation (Caz) that cannot bind metal ions (*42*). Relative to metal-bound forms, the latter is less stable and more permeable to quenchers such as acrylonitrile and acrylamide (*14*, *21*). The phosphorescence decay of azurin is uniform with τ_0 values of 0.40 and 1.93 s at 25 and -5 °C, respectively, for Znaz and τ_0 values of 0.24 and 1.81 s at 25 and -5 °C, respectively, for Caz. Besides investigating quenching by HA, BA, TA, and SA, we also re-examined O_2 and acrylamide quenching under the same temperature and solvent conditions.

Up to quenching rates of $\leq 10^4$ s^{-1} or Q concentrations of $\leq$1 M, the Stern–Volmer plots were found to be linear with respect to Q concentration, throughout. We point out that the saturation effect reported earlier for acrylamide quenching of Cd-azurin at $>$0.25 M Q (*14*) was not observed. The quenching rate constants and the respective $\Delta H^{\ddagger}(k_q)$ values are listed in Table 2, and the two parameters are conveniently displayed in Figure 5B. The results show a dramatic inverse dependence of k_q on Q size with both azurin forms, and a total inhibition of the reaction with the largest Q forms. For Znaz, k_q decreases by 7 orders of magnitude from O_2 to acrylamide, the reaction with the latter being barely detectable on the second time scale. No quenching is observed with TA and SA. Further, the modest decrease in τ for HA and BA is most probably owed to quenching impurities in commercial stocks. Indeed, the low $\Delta H^{\ddagger}(k_q)$ value ($<$5 kcal/mol) associated with HA and BA quenching of Znaz is not consistent with a penetration mechanism [$\Delta H^{\ddagger}(k_q) \approx$ 10 kcal/mol for the smallest quencher, O_2] and supports the hypothesis of through-space interactions with trace impurities in the solvent. The inability of acrylamide derivatives to penetrate the protein interior, even on the second time scale, suggests a Q size threshold of $\sim$70 for solutes gaining access to this protein core.

For the less stable metal-free Caz, there is a general increase in k_q values with respect to Znaz, indicating either a more flexible fold of the apoprotein or the opening of additional quencher migration pathways through a vacant metal binding pocket. For acrylamide, k_q increases more than 40-fold, while for HA and BA, quenching now becomes detectable (Figure 5B and Table 2). $\Delta H^{\ddagger}(k_q)$ of the apoprotein increases from 9.4 kcal/mol with O_2 to 17.7 kcal/mol with acrylamide, the barrier remaining high also for HA and BA. It decreases abruptly to $\sim$5 kcal/mol for TA and SA, the small magnitude suggesting again that access to the largest Q forms is denied and that the residual reaction is probably due to impurities.

Alkaline Phosphatase. Trp-109 of dimeric AP is the most internal Trp residue of the protein set. It is buried 1.1 nm below the molecular surface, within a tight and rigid local structure (*43*),

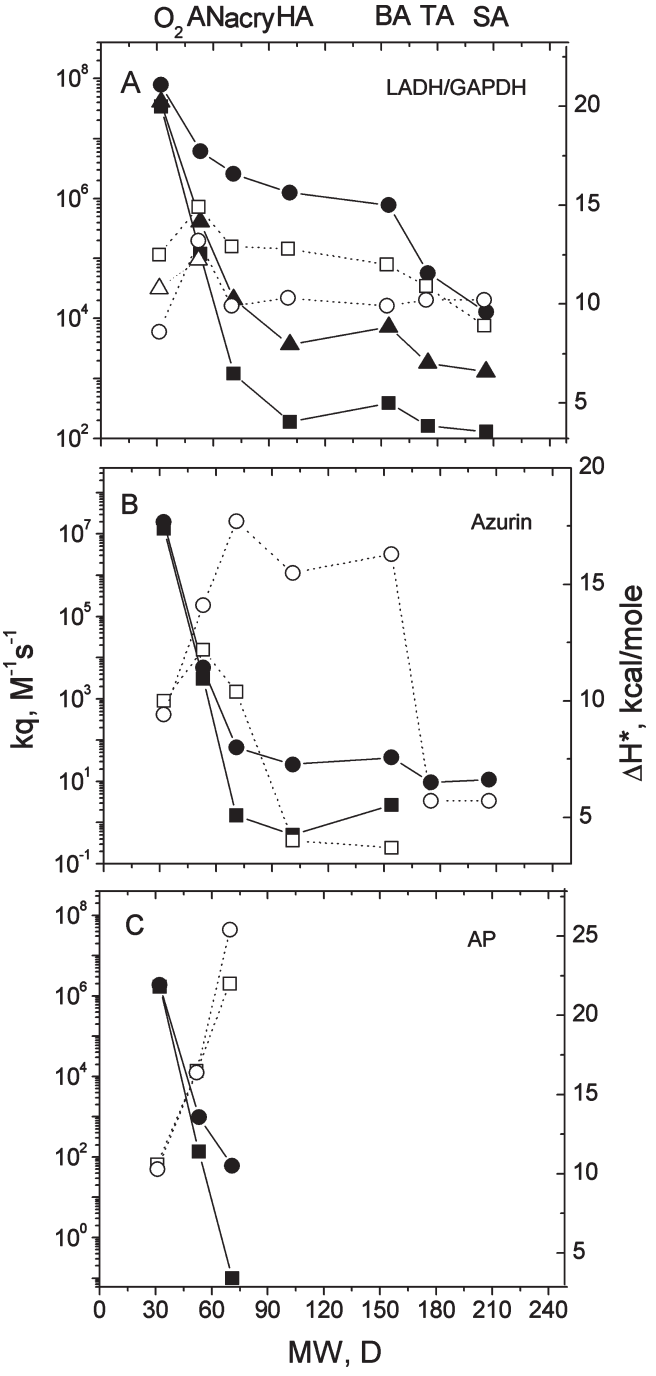

FIGURE 5: Dependence of the quenching rate constant (k_{qmax} in the case of LADH) on quencher M_w, at 25 °C (data from Table 2): (A) LADH (▲), LADH–ADPR (■), and GAPDH (●), (B) Znaz (■) and Caz (●), and (C) AP (■) and mdAP (●). Denoted with empty symbols joined by a dotted line is the corresponding activation enthalpy, $\Delta H^{\ddagger}(k_q)$. The data for acrylonitrile (AN) are from ref *21*.

as evidenced by an exceptionally long phosphorescence lifetime (τ_0 = 1.75 s at 25 °C and 3.18 s at -5 °C). Removal of Zn^{2+} from AP generates a less stable more flexible fold (mdAP) in which the phosphorescence lifetime of Trp-109 is reduced to 19.4 ms at 25 °C and 91 ms at -5 °C (*39*). We investigated quenching by HA, BA, TA, and SA and re-examined O_2 and acrylamide quenching under the same temperature and solvent conditions.

The magnitudes of k_q values derived from the gradient of linear Stern–Volmer plots are collected in Table 2 and displayed in Figure 5C. The results demonstrate that in both AP and mdAP the site of Trp-109 is accessible to only O_2 and acrylamide (and to

intermediate size acrylonitrile) in that no quenching was detected from the larger acrylamide derivatives. As with azurin, diffusive migration of these solutes to the protein core is a steep function of molecular size with an apparent threshold around the molecular weight of acrylamide. In the native protein, k_q equals 1.7×10^6 M^{-1} s^{-1} for O_2 and decreases to 0.1 M^{-1} s^{-1} for acrylamide, both values representing the smallest quenching constants for O_2 and acrylamide observed to date in proteins. The main effects of metal removal are to increase 600-fold the acrylamide quenching rate and to increase the activation barrier by 3.4 kcal/mol. The implication is that in mdAP additional large amplitude structural fluctuations that enhance penetration of acrylamide into the protein interior are set free. Again, the barrier of the structural fluctuations underlying Q diffusion in both AP and mdAP increases almost linearly with Q size.

DISCUSSION

We have interpreted quenching rate constants in terms of structural fluctuations in the native fold permitting Q access to internal sites. The assumption is that contributions from alternative reaction pathways, such as long-range through-space interactions with Q in the solvent, either freely diffusing or bound to the protein surface, are negligible or clearly distinguishable. The concern about alternative quenching mechanisms grows with large quenchers such as acrylamide and derivatives for which diffusive migration may be greatly hindered. For a random Q distribution in the solvent, external quenching can be estimated applying eq 5, $k_I(r_p)$. Its validity has recently been confirmed by accounting for acrylamide quenching of the superficially buried residues of RNase T1 and parvalbumin, where external quenching dominates the reaction (*32*). On the basis of the depth of burial of the chromophore (r_p), taken from the protein crystallographic structure ($r_p = 0.45$, 0.5, 0.8, and 1.1 nm), eq 5 predicts that, for acrylamide, $k_I(r_p) = 20$, 3.7, 1.5×10^{-4}, and 5.8×10^{-9} M^{-1} s^{-1} for LADH, GAPDH, azurin, and AP, respectively. Hence, in each case, k_I makes a negligible contribution when compared to the corresponding experimental rate constant of acrylamide and derivatives (Table 2).

External quenching may become more efficient in the case of Q binding to the proximity of the chromophore, even if then the Stern−Volmer plot deviates from linearity and assumes the form of a hyperbolic binding curve. Such a behavior was indeed observed with LADH quenching by acrylamide and its larger derivatives. However, even in this case, important binding contributions to the experimental rate are effectively ruled out by the strong reduction in quenching rates in the coenzyme complex and in glycerol solutions. The sharp r dependence of $k(r)$ implies that only Q molecules bound within a small surface area around the dimer interface would be sufficiently close to interact with Trp-314. Because the local structure is the same in LADH and in the rigid LADH−ADPR complex, one would anticipate equivalent binding affinity and a similar quenching contribution from protein-bound Q molecules. Consequently, the residual quenching observed in the complex excludes important binding contributions in the free protein. Likewise, strong inhibition of acrylamide and TA quenching in glycerol solutions is in contrast with a binding model as the organic solvent, instead of lowering the binding affinity, is known to strengthen binding of acrylamide to proteins (*44*). Conversely, in a Q penetration mechanism, the anticipation is that the conformational fluctuations required for Q access will be effectively slowed in the more rigid ADPR complex and become dampened by the solvent viscous drag (*45*, *46*). Of course, marginal quenching contributions from weak, aspecific association of Q with the protein surface are more difficult to rule out, especially with superficial Trp residues. As mentioned above, a preferential Q distribution near the subunit interface region could well be responsible for the residual, roughly constant quenching rates of HA, TA, and SA in the LADH−ADPR complex and its 2-fold increase with double-headed BA.

The penetration of solutes into internal regions of the globular fold is correlated with the frequency and amplitude of structural fluctuations in the polypeptide. The gate frequency k_0 (eq 4) and the diffusing constant D_p inferred from $k_q(Q)$ (eq 3) in effect monitor the frequency of the rate-limiting structural fluctuation, with an amplitude commensurate with the size of Q, that governs the migration of Q to the interior. Indeed, in the case of eq 3, it is customary to picture migration of Q through the protein matrix as a random walk process in which Q jumps between "solvation" cages (protein cages) at a rate that is determined by the free energy barrier between cages, which in turn is the barrier of the underlying structural fluctuations creating a transient passage of suitable size between adjacent cages. Because the barriers are expected to vary considerably between regions of the macromolecule that differ in packing density and local bonding patterns, Q migration is often viewed as a sequential multistep reaction whose rate is essentially determined by crossing of the highest barrier (the slowest rate-limiting step) on its way to the chromophore. The results of this study indicate that the protein matrix is relatively permeable to O_2, the diffusion coefficient being reduced by at most a factor of 3×10^3 relative to that of diffusion in water. $k_q(O_2)$ values of $> 10^6$ M^{-1} s^{-1} entail that motions of this amplitude occur on the submicrosecond time scale and shorter time scales. The relatively narrow range of O_2 quenching rate constants among the four protein sites, a factor of 40 between superficial regions (LADH and GAPDH) and deep compact cores (azurin and AP), demonstrates that motions of this amplitude range pervade the globular fold and are only slightly sensitive to the degree of burial or to the local secondary and tertiary structure. That is also supported by the relative invariance of $k_q(O_2)$ upon modulation of structural flexibility, as induced by formation of a complex in LADH or metal binding in azurin and AP. The penetration of O_2 is characterized by a relatively low and constant activation barrier [$\Delta H^{\ddagger}(k_q) \leq 10$ kcal/mol], which is just twice the barrier to diffusion in water. Apparently, folded polypeptides do not oppose a strong barrier to passive internal diffusion of small neutral solutes like atoms and diatomic molecules.

Diffusive migration is considerably slowed with larger Q species, although the extent varies markedly among the four proteins examined. The k_q versus Q size profiles of Figure 5 distinguish neatly deep cores from more superficial regions of the macromolecule. With the compact cores of azurin and AP, the increment in size from O_2 to acrylonitrile and to acrylamide causes a roughly exponential decrease in the penetration rate, amounting to an overall factor of 10^7 for azurin and 1.7×10^7 for AP. In these proteins, acrylamide represents a size threshold to solute penetration of the deep interior in that access to the larger acrylamide derivatives is totally inhibited on the second time scale. The large amplitude motions that permit acrylamide diffusion in these proteins occur in the 0.1−10 s^{-1} frequency range and exhibit relatively large activation barriers, ~20−25 kcal/mol.

With regard to activation barriers to diffusion of solutes in Caz, AP, and mdAP, we note a direct, inverse correlation between the protein frictional drag and barrier height. In fact, a roughly exponential decrease in k_q with Q size (Figure 5B,C) is largely ascribed to a linear increase in $\Delta H^{\ddagger}(k_q)$ (from 10.6 to 22−25 kcal/mol). While it is reasonable that larger amplitude motions involve higher activation barriers, such a linear relationship between amplitude and barrier height, if not accidental, may be an intrinsic feature of well-packed domains.

Contrary to azurin and AP, the access of acrylamide derivatives is permitted to the more superficial sites ($r_p = 0.45-0.5$ nm) of LADH and GAPDH, where k_q decreases much more gradually with Q size (Figure 5A). When Q doubles in size, from O_2 to acrylamide, k_q decreases by merely factors of 30 with GAPDH and 2×10^3 with LADH. Remarkably, a further 3-fold increase in Q size, from acrylamide to SA, causes a reduction in k_q of only 200-fold with GAPDH and 16-fold with LADH. For the largest Q species, we are dealing with structural fluctuations of frequencies that exceed 10^4 s^{-1} in GAPDH and are on the order of 100 s^{-1} in LADH, motions that in both proteins are characterized by a relatively low activation barrier (8−10 kcal/mol). Although in this case we are probing rather superficial sites, this need not be a general trend as there are indications that such large amplitude motions are not ubiquitous in external regions. Indeed, acrylamide quenching of RNase T1 and parvalbumin, in which the Trp residue is barely 0.2 nm from the aqueous interface, is 45- and 76-fold slower, respectively, than in GAPDH, and the actual rate of penetration of acrylamide into these sites is even smaller than that inferred from k_q because in these proteins the reaction is dominated by external quenching (*32*).

An apparently general feature of large amplitude motions, in both shallow and deep regions of the globular fold, is the particular sensitivity to frequency modulation by ligand binding as well as by solvent viscosity. Thus, binding of ADPR to LADH and the increase in solvent viscosity in glycerol solutions reduce by more than 10-fold the level of internal migration of acrylamide and larger derivatives. Similarly, removal of Zn from the native protein increases k_q(acrylamide) by 44-fold in azurin and 600-fold in AP. In comparison, the corresponding changes in k_q become progressively smaller with acrylonitrile and O_2.

The ready penetration of large Q forms in LADH and GAPDH raises the question of whether this characteristic can be traced to a particular local folding pattern. Inspection of crystallographic structures allows speculation about possible migration pathways. W84 in GAPDH exhibits an unusually high accessibility to both small and large solutes. The weak size discrimination of penetration rates and the prompt access of charged solutes like SA, which are normally relegated to the aqueous phase, suggest that the underlying structural fluctuations must transiently expose the chromophore to the aqueous environment or to its proximity. Its crystallographic structure (*38*) shows that W84 lies at the bottom of a large cleft, shielded from the solvent by the side chains of V28 and I87, lining one side of the cleft, and by I72 on the opposite side. K3 and K74 are placed at the two extremes of the cleft (Figure 6). All these side chains are anchored to coil segments of the polypeptide and exhibit larger than average *B* factors, suggestive of a good degree of conformational freedom. Q diffusion could involve either a local displacement of side chains, opening a channel to the solvent, or a more extended or partial unfolding transition bringing buried W84 to the surface. Simple inspection shows that the side chain pair of I72 and I87 may act as a gate to solute diffusion inside the cleft, as

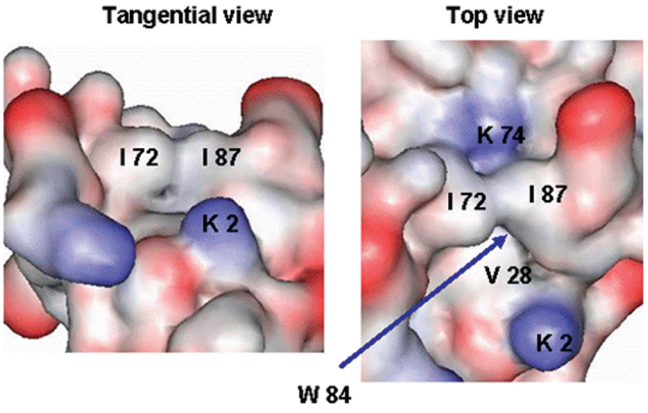

FIGURE 6: Top and tangential views (Viewer Lite) of the surface cleft above W84 of GAPDH illustrating the position of the side chains of I72, I87, and V28, presiding over the proposed access route of large quenchers to the vicinity of the aromatic residue.

a concerted rotational displacement would create a large water channel practically connecting W84 to the solvent. Because the rotation of superficial side chains is expected to be a low-barrier rapid motion, such a pathway would readily account for both rapid Q access and a relatively small (≈10 kcal/mol), constant activation barrier for the penetration of acrylamide and its derivatives. The alternative scenario of a partial unfolding transition is less likely. The site of W84 is sandwiched between a large β-sheet and an α-helix, and the transition would require breaking of stable secondary structures, which is far more costly in terms of free energy than the rotation of superficial side chains.

The size dependence of quenching rates of acrylamide derivatives is even weaker for W314 of LADH (Figure 5A). Here, the probe is located at the dimer subunit interface, and a previous detailed analysis of acrylamide quenching proposed that access of the quencher to the site occurred by two distinct protein-gated pathways: a high-frequency gate (11800 s^{-1}) with a σ of 0.95 M involving the rotation of side chains (V276 and L307) and a low-frequency gate (40 s^{-1}) with a σ of 0.004 M represented by transient opening of subunit contacts between the K315 and T313 pair in opposite subunits (*19*). The quenching behavior of the larger acrylamide derivatives is again consistent with protein-gated diffusion except that now a single slow gate is sufficient to account for all the data. Both frequency ($k_0 \approx 100$ s^{-1}) and midpoint saturation (0.018−0.075 M) associate it with the slow gate proposed for acrylamide penetration, suggesting that the fast gate is virtually precluded to solutes larger than acrylamide. Fluctuations of subunit contacts can indeed give rise to relatively large amplitude motions and explain the poor selectivity of migration rates with regard to Q size and charge. As noted, the main effect of increasing Q size is to increase the concentration of midpoint gate saturation, from 4 mM acrylamide to 75 mM SA, which is likely a consequence of less efficient quenching of the open gate configuration by larger solutes that may diffuse more slowly to or approach less closely the aromatic probe. The gate frequency is sharply reduced in the LADH−ADPR complex and in viscous glycerol solutions, effectively blocking access to the large acrylamide derivatives. These responses are in accord with the substantial tightening of the subunit interface region in the binary complex, revealed by the increase in the phosphorescence lifetime of W314, and the expected dampening of structural fluctuations in proteins by viscous drag of the solvent (*45*, *46*). In addition to viscosity-dependent kinetic effects on the quenching rate, opening of the subunit interface may be further inhibited by

the selective stabilization of closed, compact protein conformers by a cosolvent known to promote folding and subunit association (*47*).

In summary, this study shows that high-frequency small amplitude motions pervade protein folds, permitting relatively unhindered diffusion of neutral diatomic molecules deep down to the compact core of the macromolecule. It also points out that larger amplitude motions that permit access of large solutes to inner regions may exhibit vastly different frequencies among protein sites. In the sample proteins examined, the rate of diffusion of solutes through homogeneous compact domains decreased exponentially with molecular size, whereas in more superficial regions of the globular fold, unexpectedly large amplitude, low-barrier fluctuations permitted the shallow penetration of even bulky solutes. The method, by disclosing the amplitude range of protein motions over a wide time scale, can shed light on protein dynamics up to the millisecond to second time domain where information is scarce. Of particular interest will be the enquiry into slow structural fluctuations visiting rarely populated conformational substates of the protein ensemble that are beyond detection by most biophysical techniques. The method relies on a natural probe that in principle can be placed in strategic regions of the macromolecule for the examination of the local dynamics even under nativelike conditions.

SUPPORTING INFORMATION AVAILABLE

SDS−PAGE of LADH used in these experiments (Figure S1) and Stern−Volmer plots relative to oxygen quenching of Trp phosphorescence in the proteins GAPDH, LADH, Caz, and AP (Figure S2). This material is available free of charge via the Internet at http://pubs.acs.org.

REFERENCES

1. Eppler, R. K., Hudson, E. P., Chase, S. D., Dordick, J. S., Reimer, J. A., and Clark, D. S. (2008) Biocatalyst activity in nonaqueous environments correlates with centisecond-range protein motions. *Proc. Natl. Acad. Sci. U.S.A. 105*, 15672–15677.
2. Frederick, K. K., Marlow, M. S., Valentine, K. G., and Wand, A. J. (2007) Conformational entropy in molecular recognition by proteins. *Nature 448*, 325–329.
3. Hammes-Schiffer, S., and Benkovic, S. J. (2006) Relating protein motion to catalysis. *Annu. Rev. Biochem. 75*, 519–541.
4. Henzler-Wildman, K., and Kern, D. (2007) Dynamic personalities of proteins. *Nature 450*, 964–972.
5. Kale, S., Ulas, G., Song, J., Brudvig, G. W., Furey, W., and Jordan, F. (2008) Efficient coupling of catalysis and dynamics in the E1 component of *Escherichia coli* pyruvate dehydrogenase multienzyme complex. *Proc. Natl. Acad. Sci. U.S.A. 105*, 1158–1163.
6. Persson, E., and Halle, B. (2008) Nanosecond to microsecond protein dynamics probed by magnetic relaxation dispersion of buried water molecules. *J. Am. Chem. Soc. 130*, 1774–1787.
7. Wand, A. J. (2001) Dynamic activation of protein function: A view emerging from NMR spectroscopy. *Nat. Struct. Biol. 8*, 926–931.
8. Bouvignies, G., Bernado, P., Meier, S., Cho, K., Grzesiek, S., Bruschweiler, R., and Blackledge, M. (2005) Identification of slow correlated motions in proteins using residual dipolar and hydrogen-bond scalar couplings. *Proc. Natl. Acad. Sci. U.S.A. 102*, 13885–13890.
9. Bustamante, C. (2008) In singulo biochemistry: When less is more. *Annu. Rev. Biochem. 77*, 45–50.
10. Mittermaier, A., and Kay, L. E. (2006) New tools provide new insights in NMR studies of protein dynamics. *Science 312*, 224–228.
11. Lakowicz, J. R., and Weber, G. (1973) Quenching of protein fluorescence by oxygen. Detection of structural fluctuations in proteins on the nanosecond time scale. *Biochemistry 12*, 4171–4179.
12. Calhoun, D. B., Englander, S. W., Wright, W. W., and Vanderkooi, J. M. (1988) Quenching of room temperature protein phosphorescence by added small molecules. *Biochemistry 27*, 8466–8474.
13. Calhoun, D. B., Vanderkooi, J. M., and Englander, S. W. (1983) Penetration of small molecules into proteins studied by quenching of phosphorescence and fluorescence. *Biochemistry 22*, 1533–1539.
14. Cioni, P., and Strambini, G. B. (1998) Acrylamide quenching of protein phosphorescence as a monitor of structural fluctuations in the globular fold. *J. Am. Chem. Soc. 120*, 11749–11757.
15. Cioni, P., and Strambini, G. B. (1999) Pressure/temperature effects on protein flexibilty from acrylamide quenching of protein phosphorescence. *J. Mol. Biol. 291*, 955–964.
16. Saviotti, M. L., and Galley, W. C. (1974) Room temperature phosphorescence and the dynamic aspects of protein structure. *Proc. Natl. Acad. Sci. U.S.A. 71*, 4154–4158.
17. Strambini, G. B. (1987) Quenching of alkaline phosphatase phosphorescence by O_2 and NO. Evidence for inflexible regions of protein structure. *Biophys. J. 52*, 23–28.
18. Strambini, G. B., and Cioni, P. (1999) Pressure-temperature effects on oxygen quenching of protein phosphorescence. *J. Am. Chem. Soc. 121*, 8337–8344.
19. Strambini, G. B., and Gonnelli, M. (2009) Acrylamide quenching of Trp phosphorescence in liver alcohol dehydrogenase: Evidence of gated quencher penetration. *Biochemistry 48*, 7482–7491.
20. Vanderkooi, J. M. (1991) Topics in Fluorescence Spectroscopy. In Biochemical Applications (Lakowicz, J. R., Ed.) pp 113−116, Plenum, New York.
21. Strambini, G. B., and Gonnelli, M. (2010) Acrylonitrile quenching of Trp phosphorescence in proteins: A probe of the internal flexibility of the globular fold. *Biophys. J. 99*, 944–952.
22. Gonnelli, M., and Strambini, G. B. (1995) Phosphorescence Lifetime of Tryptophan in Proteins. *Biochemistry 34*, 13847–13857.
23. Karlsson, B. G., Pascher, T., Nordling, M., Arvidsson, R. H., and Lundberg, L. G. (1989) Expression of the blue copper protein azurin from *Pseudomonas aeruginosa* in *Escherichia coli*. *FEBS Lett. 246*, 211–217.
24. Henis, Y. I., and Levitzki, A. (1977) The role of the nicotinamide and adenine subsites in the negative co-operativity of coenzyme binding to glyceraldehyde-3-phosphate dehydrogenase. *J. Mol. Biol. 117*, 699–716.
25. van de Kamp, M., Silvestrini, M. C., Brunori, M., Van Beeumen, J., Hali, F. C., and Canters, G. W. (1990) Involvement of the hydrophobic patch of azurin in the electron-transfer reactions with cytochrome C551 and nitrite reductase. *Eur. J. Biochem. 194*, 109–118.
26. Strambini, G. B., and Gabellieri, E. (1991) Phosphorescence from Trp-48 in Azurin: Influence of Cu(Ii), Cu(I), Ag(I), and Cd(Ii) at the Coordination Site. *J. Phys. Chem. 95*, 4352–4356.
27. Strambini, G. B., Kerwin, B. A., Mason, B. D., and Gonnelli, M. (2004) The triplet-state lifetime of indole derivatives in aqueous solution. *Photochem. Photobiol. 80*, 462–470.
28. Cioni, P., Gabellieri, E., Gonnelli, M., and Strambini, G. B. (1994) Heterogeneity of Protein Conformation in Solution from the Lifetime of Tryptophan Phosphorescence. *Biophys. Chem. 52*, 25–34.
29. Sillen, A., and Engelborghs, Y. (1998) The Correct Use of "Average" Fluorescence Parameters. *Photochem. Photobiol. 65*, 475–486.
30. Owen, C. S., and Vanderkooi, J. M. (1991) Diffusion-dependent and -independent collisional quenching of fluorescence and phosphorescence. *Comments Mol. Cell. Biophys. 7*, 235–257.
31. Wright, W. W., Owen, C. S., and Vanderkooi, J. M. (1992) Penetration of analogues of H_2O and CO_2 in proteins studied by room temperature phosphorescence of tryptophan. *Biochemistry 31*, 6538–6544.
32. Strambini, G. B., and Gonnelli, M. (2010) Protein phosphorescence quenching: Distinction between quencher penetration and external quenching mechanisms. *J. Phys. Chem. B 114*, 9691–9697.
33. Vanderkooi, J. M., Englander, S. W., Papp, S., Wright, W. W., and Owen, C. S. (1990) Long-Range Electron Exchange Measured in Proteins by Quenching of Tryptophan Phosphorescence. *Proc. Natl. Acad. Sci. U.S.A. 87*, 5099–5103.
34. Eklund, H., Samama, J. P., and Jones, T. A. (1984) Crystallographic investigations of nicotinamide adenine dinucleotide binding to horse liver alcohol dehydrogenase. *Biochemistry 23*, 5982–5996.
35. Strambini, G. B., and Gonnelli, M. (1990) Tryptophan Luminescence from Liver Alcohol Dehydrogenase in Its Complexes with Coenzyme: A Comparative Study of Protein Conformation in Solution. *Biochemistry 29*, 196–203.
36. Theorell, H., and Tatemoto, K. (1971) Thermal stability of horse liver alcohol dehydrogenase and its complexes. *Arch. Biochem. Biophys. 143*, 354–358.
37. Colonna-Cesari, F., Perahia, D., Karplus, M., Eklund, H., Braden, C. I., and Tapia, O. (1986) Interdomain motion in liver alcohol

dehydrogenase. Structural and energetic analysis of the hinge bending mode. *J. Biol. Chem. 261*, 15273–15280.
38. Skarzynski, T., Moody, P. C., and Wonacott, A. J. (1987) Structure of holo-glyceraldehyde-3-phosphate dehydrogenase from *Bacillus stearothermophilus* at 1.8 Å resolution. *J. Mol. Biol. 193*, 171–187.
39. Gonnelli, M., and Strambini, G. B. (2009) No effect of covalently linked poly(ethylene glycol) chains on protein internal dynamics. *Biochim. Biophys. Acta 1794*, 569–576.
40. Nar, H., Messerschmidt, A., Huber, R., van de Kamp, M., and Canters, G. W. (1991) Crystal structure analysis of oxidized *Pseudomonas aeruginosa* azurin at pH 5.5 and pH 9.0. A pH-induced conformational transition involves a peptide bond flip. *J. Mol. Biol. 221*, 765–772.
41. Nar, H., Messerschmidt, A., Huber, R., van de Kamp, M., and Canters, G. W. (1992) Crystal structure of *Pseudomonas aeruginosa* apo-azurin at 1.85 Å resolution. *FEBS Lett. 306*, 119–124.
42. Sandberg, A., Leckner, J., and Karlsson, B. G. (2004) Apo-azurin folds via an intermediate that resembles the molten-globule. *Protein Sci. 13*, 2628–2638.
43. Sowadski, J. M., Handschumacher, M. D., Murthy, H. M., Foster, B. A., and Wyckoff, H. W. (1985) Refined structure of alkaline phosphatase from *Escherichia coli* at 2.8 Å resolution. *J. Mol. Biol. 186*, 417–433.
44. Punyczki, M., Norman, J. A., and Rosenberg, A. (1993) Interaction of acrylamide with proteins in the concentration range used for fluorescence quenching studies. *Biophys. Chem. 47*, 9–19.
45. Gavish, B. (1980) Position-dependent viscosity effect on rate coefficient. *Phys. Rev. Lett. 44*, 1160–1163.
46. Gavish, B., and Werber, M. M. (1979) Viscosity-dependent structural fluctuations in enzyme catalysis. *Biochemistry 18*, 1269–1275.
47. Gekko, K., and Timasheff, S. N. (1981) Thermodynamic and kinetic examination of protein stabilization by glycerol. *Biochemistry 20*, 4677–4686.